# PLASMA CONFINEMENT IN THE GAMMA 10 TANDEM MIRROR

K.YATSU, L.G.BRUSKIN, T.CHO, M.HAMADA, M.HIRATA, H.HOJO,
M.ICHIMURA, K.ISHII, A.ITAKURA, I.KATANUMA, Y.KIWAMOTO,
J.KOHAGURA, S.KUBOTA, A.MASE, Y.NAKASHIMA, T.SAITO,
Y.SAKAMOTO, T.TAMANO, Y.TATEMATSU, T.TOKUZAWA, M.YOSHIKAWA
Plasma Research Center, University of Tsukuba, Tsukuba, Ibaraki 305-8577, Japan

**Abstract**

The central-cell density and the diamagnetic signal were doubled due to plug potential formation by ECRH in the hot ion mode experiments on the GAMMA 10 tandem mirror. In order to obtain these remarkable results, the axisymmetrized heating patterns of ECRH and ICRF were optimized. Furthermore, conducting plates were installed adjacent to the surface of the plasma along the flat shaped magnetic flux tube located at the anchor transition regions; the plates may contribute to reduce some irregular electric fields produced possibly with ECRH in these thin flux tube regions. The conducting plates contributed to the reduction of the radial loss rate to be less than 3% of the total particle losses along with the improvements in the reproducibility of the experiments and the controllability of the potential confinement. The increases in the central-cell density and the diamagnetism in association with the increase in the plug potentials scaled well with increasing the ECRH powers. A plug potential of 0.6 kV and a density increase of 100% were achieved using an ECRH power of 140 kW injected into both plug regions. The plasma confinement was improved by an order of magnitude over a simple mirror confinement due to the tandem mirror potential formation.

## 1. INTRODUCTION

In the GAMMA 10 tandem mirror, plug and thermal barrier potentials of 1.7 kV and 1.1 kV were attained with an energy confinement time of 0.6 sec [1,2]. Following the results in this plasma operational mode, recent GAMMA 10 experiments have been carried out for the purpose of further increase in ion temperatures and densities by an ion cyclotron range of frequency (ICRF) heating associated with potential pluggings due to electron cyclotron resonance heatings (ECRH). The increase in the ICRF heating power sources along with the suitable adjustment of the ICRF heating powers on the type III and double half-turn antennas, improved ion temperatures to be 10 keV with $\beta$=6% [3]. This operational mode is hereafter referred to as a hot ion mode. In the hot ion mode, plasma was sustained by the ICRF heating with gas puffing in the central cell. Positive plug potentials were formed in the axisymmetric end mirror cells by an application of a fundamental ECRH to the ICRF sustained plasma. However, a density increase due to the potential confinement was less than 10% [3]. After the recent optimizations of the axisymmetrized heating patterns of ECRH and ICRF heating powers achieved a density increase of 50% [4].

The improvement of plasma confinement in the hot ion mode was studied with a newly developed end loss ion energy analyser (ELA), which can completely eliminate the signal disturbance from high energy electrons and can directly obtain the energy spectra of end loss ions [5]. The potential confinement of passing ions was clearly shown by the waveforms of end-loss currents as well as their energy spectra. For the potential confinement in the hot ion mode, some radial losses of passing ions were observed. A radial loss rate of the passing ions was measured by analysing end loss currents under the condition with a single ended plugging. Though the radial loss rate was usually several percents, a shot with an estimated radial loss rate of less than 3% was obtained.

In addition to the optimizations of ECRH and ICRF heating, conducting plates have been installed in the anchor transition regions to fix the potential at the plasma boundary, thereby reducing possible irregular electric fields, which were considered to be a cause of the radial loss. Experiments have been carried out during a 6 month period with the conducting plates. Improvements in the reproducibility and controllability of the potential confinement experiments

have been obtained. The central cell density and diamagnetic signal were doubled with the potential confinement after the installation of the conducting plates.

## 2. THE GAMMA 10 TANDEM MIRROR

The GAMMA 10 tandem mirror consists of a central cell, two anchor cells and two end mirror cells. The anchor cells with a minimum B configuration locate at both ends of the central cell and are connected to the end mirror cells. Ions in the central cell are heated by a slow ion cyclotron wave excited by a pair of double half-turn antennas installed near both ends of the central cell. Ions in the anchor cells are also heated by another ion cyclotron wave with a frequency different from that in the central cell. The plasma is initiated by magneto-plasma-dynamic (MPD) plasma guns located at the both ends. The plasma is sustained by ICRF heating with gas puffing in the central cell. Positive plug potentials are formed in the axisymmetric end mirror cells by fundamental ECRH.

For plasma diagnostics, the followings are mainly used. Plasma densities are measured with microwave interferometers at several locations along GAMMA 10. End loss currents and ion energy spectra at the ends are measured with the newly developed end loss ion energy analysers (ELA) [5]. Plasma potentials in the central cell and in the barrier region are measured with heavy ion beam probes [6]. The plasma potentials in the plug regions are determined by the energy analysis of end loss ions measured with the ELA. The plasma confinement potential is determined as the potential difference between the plug region and the central cell. The ion temperature is determined from the data using a charge-exchange neutral-particle energy analyser together with the diamagnetic signal. The electron temperature is obtained from x-ray diagnostics. Several types of x-ray diagnostics, such as x-ray spectrum analysis, x-ray absorption methods, and x-ray tomographic reconstructions using semiconductor detectors, as well as microchannel plates have been employed for obtaining electron velocity distribution functions and their spatial variations. The atomic hydrogen Hα emission is observed radially and axially to determine the ionization rate: this system is absolutely calibrated using an NIST tungsten lamp.

## 3. POTENTIAL CONFINEMENT IN GAMMA 10

### 3.1 Potential confinement and radial loss

In GAMMA 10 experiments, an ICRF sustained plasma was at first produced. The ICRF heatings in the central cell and anchor cells with gas puffing in the central cell sustains a hot ion plasma with an ion temperature and plasma density of about 4 keV and $2\times10^{12}$ $cm^{-3}$, respectively. The ion temperature in the central cell was anisotropic with a ratio of the perpendicular to parallel temperature of around 10. No major radial particle loss was observed with the ICRF sustained plasma. After the plasma reached a steady state, ECRH is applied to the plug region for producing the plug potential. Only fundamental ECRH at the plug was used in these experiments.

Potential confinement was studied under various heating scenarios such as without ECRH, ECRH at one end, and ECRH at both ends. Figure 1(a) illustrates the axial magnetic field strength and locations of the heating systems used in this experiment. The waveforms of ion end loss currents and central-cell line densities are shown in Figs.1(b) and (c), where NLCC denotes the central-cell line density, and E-ELA and W-ELA indicate end loss current to the east and west ends. When ECRH is applied only to the west plug, the ion current to the west ELA (W-ELA) decreases due to the potential reflection of low energy ions, while the ion current to the east ELA (E-ELA) increases due to the ions reflected by the west plug potential; NLCC does not increase. When ECRH is applied to both plugs, NLCC increases due to potential confinement.

Another evidence of potential confinement was given by an analysis of the end loss ion energy. Figures 2(a) and (b) show the waveforms of the central-cell line density and the end loss current for a shot with potential confinement. Figure 2(c) shows the energy distributions of end loss ions at four different times [see the same labels in Figs. 2(b) for identifying the observation times].

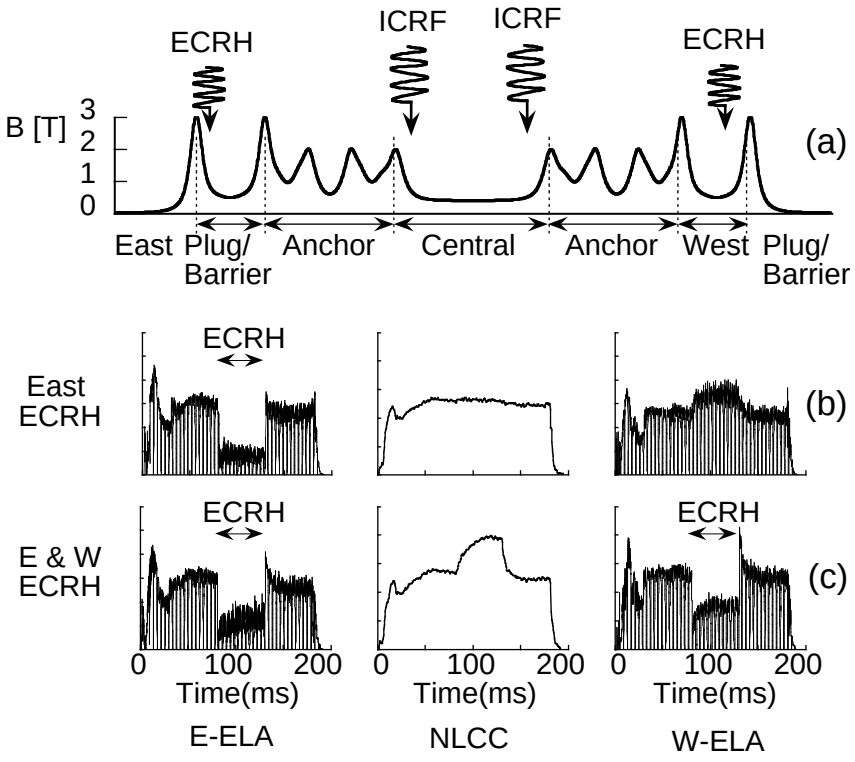


*FIG.1 (a) Axial magnetic field strength and location of heating systems. (b) to (c) Central cell line densities (NLCC) and end loss currents to the east (E-ELA) and to the west (W-ELA), where one division of NLCC is $10^{13}$ $cm^{-2}$ and that of ELA is $10^{-4}$ $A/cm^2$. ECRH is applied from 80 ms to 130 ms.*

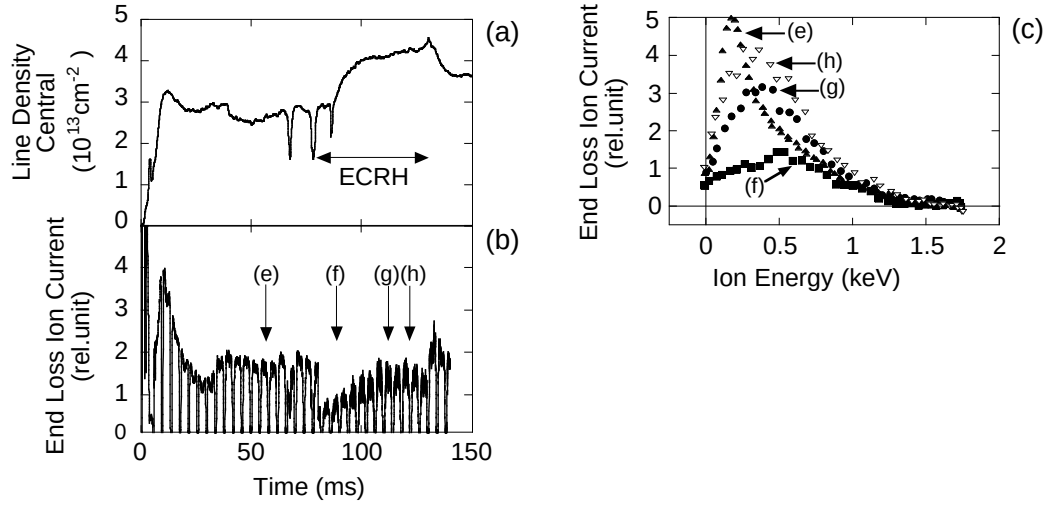


*FIG.2 Central cell line density (a), end-loss current (b), and energy distributions of end loss ions (c) where (e), (f), (g), and (h) correspond to the instants indicated in Figure (b).*

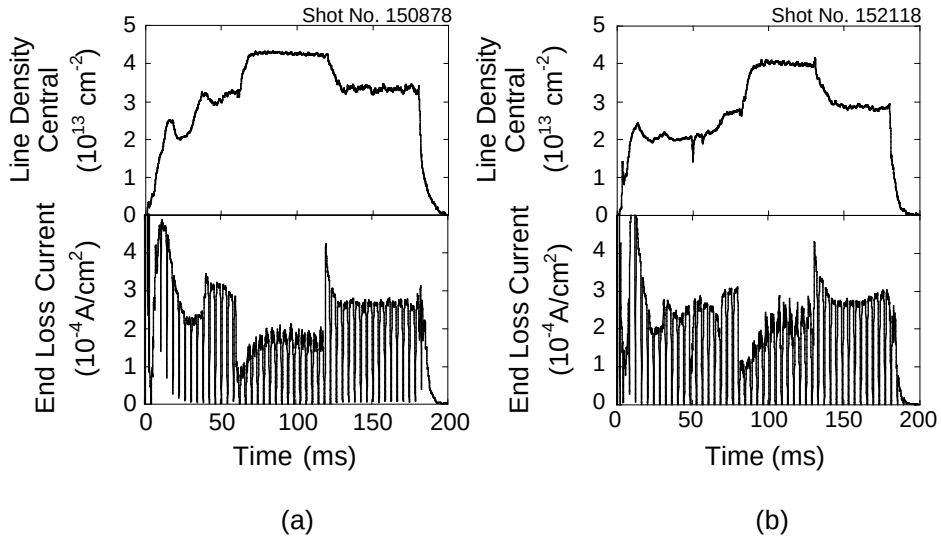


*FIG.3 (a) Wave forms of the central-cell line density and end-loss current for a shot with the density increase of 30%. (b) Wave forms of the central-cell line density and end-loss current for a shot with the density increase of 50%.*

The energy distribution of the ICRF sustained plasma is shown by (e). The ion temperature is 0.35 keV, which is about one tenth of the central-cell ion temperature. The high energy ions in the central cell are lost mainly by charge exchange loss before they are scattered into the loss cone, because of their large temperature anisotropy. At the time (f) just after the potential formation, the low energy portion disappears because the low energy ions are potentially confined. The confining potential is approximately determined as the potential difference corresponding to the peak energy of the distribution in (f) and the peak energy in (e) of Fig. 2(b). At the latter times (g) and (h), the confining potential decreases. However, it can be seen on the energy distributions at (g) and (h) that the higher energy portion increases compared with the distribution at (e). This indicates an increase in the ion temperature during potential confinement.

Figure 3(a) shows waveforms of the central-cell line density and end-loss current for a shot with a density increase of 30%. The end loss current decreases after formation of a confining potential by ECRH and then gradually increases. When ECRH is turned off, a short burst appears in the end loss current due to axial drain of the potentially confined plasma. The waveform of the end loss current, together with the waveform of the central-cell line density, indicates plasma confinement by the potential. However, the steady state end-loss current that occurs during ECRH is smaller than the current occurring before and after ECRH. Plasma production near the axis determined from Hα measurement does not change much during ECRH. Therefore, smaller end-loss current during ECRH suggests some radial losses of the potentially confined plasma. A radial loss rate was determined from a single ended plugging data such as shown in Fig. 1(b). From the measurements of the decrement and the increment of the end loss currents at both ends, we obtained a radial loss rate of passing ions, that is, a rate of the radial loss of passing ions during their passage through the anchor and plug/barrier cells. The radial loss rate corresponding to the shot shown in Fig. 3(a) is 9%. Under another experimental condition, a smaller radial loss rate of less than 3% was obtained for the shot shown in Fig. 3(b). In this shot, the lack of the end loss current during ECRH was smaller than the shot in Fig. 3(a) and the increase in the central-cell line density was 50%.

### 3.2 Installation of anchor conducting plate

The mechanism of the radial loss and the region where the loss takes place have not been identified; however, we suspect the losses from the anchor transition regions. In the anchor

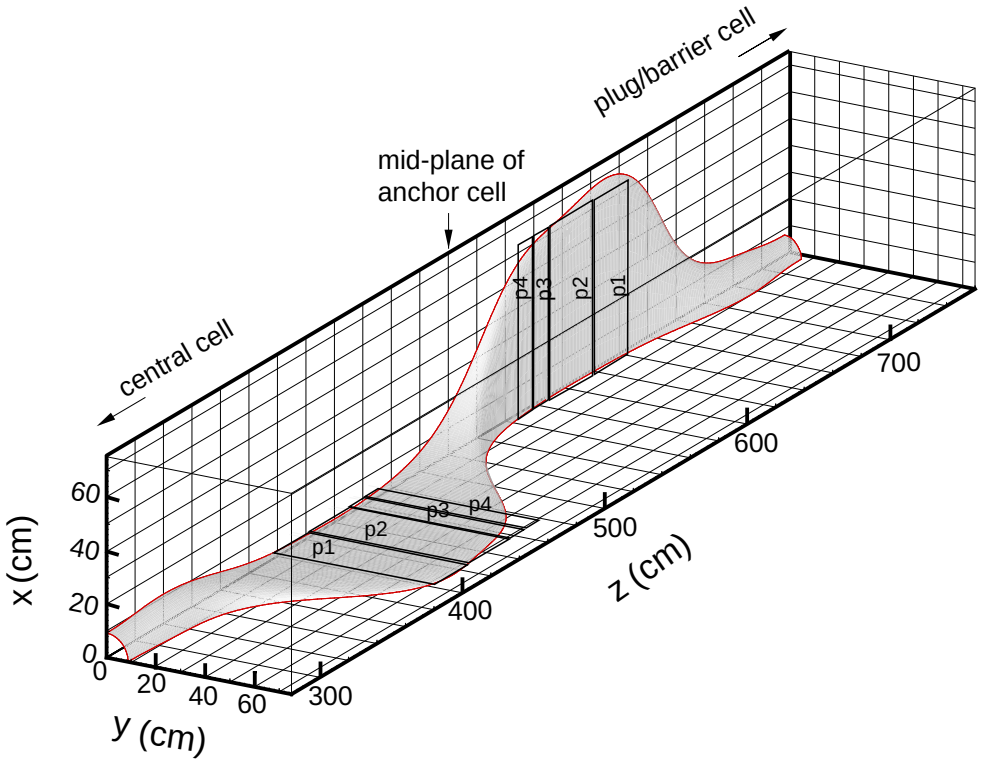


*FIG.4 A quarter of a magnetic flux tube and conducting plates in an anchor cell. The magnetic flux tube maps to a circular magnetic flux tube of 0.4 m diam. at the central cell midplane.*

transition region with fanning minimum B field, a circular magnetic flux tube of 0.4 m in diam. at the central-cell midplane maps to a 0.025m×1.4m elliptic tube. Some irregular electric fields possibly occurring with ECRH cause radial loss by **E×B** drift in the region due to the short distance across the plasma. Conducting plates were installed near the surface of the plasma in the fanning magnetic flux tube in order to fix the potential at the plasma boundary for reducing irregular electric fields. Figure 4 schematically illustrate a quarter of the conducting plates in the east anchor. The length of the plates is 124 cm and the width of P1, P2, P3, and P4 are 24.8 cm, 29.6 cm, 9.6 cm, and 7.8 cm, respectively. The spacing of each pair of conducting plates is set so as to follow the shape of the magnetic flux tube. Pairs of P1, P2, P3, and P4 are separated by 7.0 cm, 5.0 cm, 7.0 cm, and 10 cm, respectively. All plates are electrically independent. Therefore, the potential of each plate can be independently changed by changing a resistance connected to the plate.

### 3.3 Experiments with the anchor conducting plates

After the wall conditionings of the conducting plates, experiments were carried out for about 6 months. Reproducibility and controllability of experiments were improved and a larger density increase with potential confinement was obtained. The increment of the density and diamagnetism became larger with plasma shots in accordance with the progress of the wall conditioning. Figures 5(a) and (b) show the central-cell line density and diamagnetic signal, respectively. Both values are doubled by the formation of a plug potential. ECRH was applied from 80 ms to 130 ms. The duration of ECRH can be extended up to 75 ms which is the limit of the gyrotron power supply. The FWHM values of the central-cell density profiles were 16 cm before and during ECRH. The plasma density on the axis at 120 ms was $2.7\times10^{12}$ $cm^{-3}$. The diamagnetism in Fig. 5(b) is mainly due to hot ions with an average temperature of 2.8 keV. The temperature profile was more peaked than the density

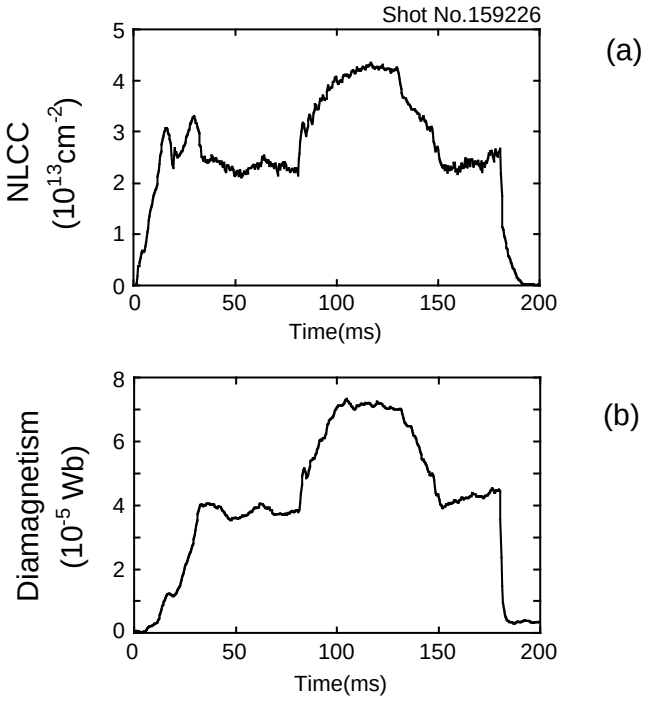


*FIG.5 Central-cell line density (a) and diamagnetic signal (b) for a shot when they are doubled by formation of a plug potential at ECRH power of 140 kW in each plug region. The plasma density on the axis at the peak line density is $2.2\times10^{12}$ $cm^{-3}$.*

profile; the temperature on the axis was 4.5 keV.

The particle confinement time of the ICRF sustained plasma was estimated as $\tau_P=eN/I$, where $e$ is the unit charge, $N$ is the total number of ions in a flux tube, and $I$ is the end loss ion current to both ends of the flux tube. The end loss currents to both ends were balanced and the end-loss current measured with the E-ELA was used to measure the particle confinement time. The plasma density in the anchor cell was nearly equal to that in the central cell, and was taken into account for the total number of ions in a flux tube. The particle confinement time was 5 ms in a flux tube located at a radius of 2 cm at the central-cell midplane. To estimate the possibility of radial losses, the particle source was evaluated from Hα measurement and compared with the end loss current measured with the ELAs for the ICRF sustained plasma. The radial loss of the ICRF sustained plasma was estimated to be much smaller than the axial loss, as far as the core plasma within the FWHM density profile was concerned. Therefore, the Hα measurement corresponded to the end loss current. By comparing the Hα measurements for plasmas with and without ECRH, the particle source during ECRH was determined. The particle confinement time for the shot shown in Fig.5 was obtained from $edN/dt=I_{ion}-I_{loss}$ where $I_{ion}$ is the equivalent ionization current, $I_{loss}$ is the loss current, because the time variation of the density has to be taken into account. The particle confinement time of 40 ms was obtained at the time 85 ms in Fig. 5(a), which is a one order of magnitude improvement due to potential confinement. The energy confinement time is obtained as $\tau_E=W/P$, where $W$ is the energy content of the plasma and $P$ is the input power of the ICRF heating. Energy confinement time of 10ms was obtained for the shot in Fig. 5. The effect of potential confinement on electrons was measured in a shot similar to the shot in Fig. 5. The electron temperature increased by 35% from 60 eV and the electron energy content increased by 70%, in accordance with the density increase during potential confinement.

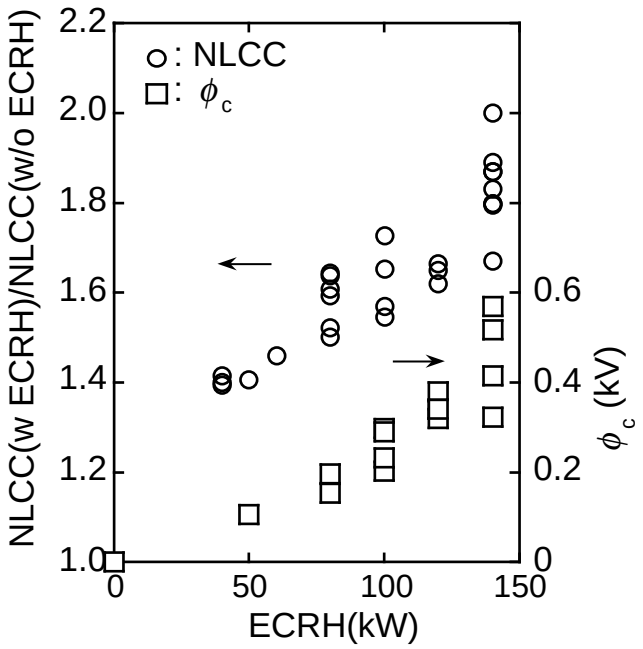


*FIG.6 Increment of the central-cell line density and the confining potential as a function of the ECRH power in each plug region.*

Figure 6 indicates the increment of the central-cell line density and the confining potential as a function of the ECRH power in each plug region. A density increase of 100% and a confining potential of 0.6 kV were obtained at an ECRH power of 140 kW. The increment of the density was larger when the conducting plate potential were floating. The floating potentials were about 400 V on the central-cell side and about 150 V on the plug/barrier cell side.

## 4. SUMMARY

The potential formation by ECRH at the plug regions and the potential confinement were clearly demonstrated by the data on the waveforms of the end loss currents with a single ended plugging and both ended pluggings. The analyses of the end loss ion energies consistently showed the evidence of the potential formation as well as the potential confinement. Suggested some amount of radial losses of the potentially confined plasma was improved to be less than 3% of the total particle losses using newly installed conducting plates in the anchor transition regions. The increases in the central-cell density and the diamagnetism in association with the increase in the plug potentials scaled well with increasing the ECRH powers. A plug potential of 0.6 kV and a density increase of 100% were achieved at the ECRH power of 140 kW. The particle and energy confinement times were improved to be 40 ms and 10 ms, respectively, due to the tandem mirror potential formation.

## REFERENCES

[1] MIYOSHI,S., et al., in Plasma Physics and Controlled Nuclear Fusion Research ( Proc. 13th Int. Conf. Washington D.C., 1990) Vol.2, IAEA, Vienna (1991) 539.
[2] MIYOSHI,S., Plasma Phys. Reports **23** (1997) 723.

[3] TAMANO,T., et al., in Plasma Physics and Controlled Nuclear Fusion Research ( Proc. 15th Int. Conf. Seville, 1994) Vol.2, IAEA, Vienna (1995) 399.
[4] YATSU,K., et al., J. Plasma and Fusion Research **74** (1998) 844.
[5] SAKAMOTO,Y, et al., Rev. Sci. Instrum. **66** (1995) 4928.
[6] ISHII,K., et al., Nucl. Fusion **30** (1990) 1051.